Cable analysis with the whole-cell patch clamp

Theory and experiment

Meyer B. Jackson
Department of Physiology, University of Wisconsin Medical School, Madison, Wisconsin 53706

ABSTRACT A theoretical analysis was undertaken of a Rall motoneuron under voltage clamp with a finite access resistance. This model is relevant to the conditions of the whole-cell patch clamp, which to date has been used very little for cable analysis. It was shown that the soma and cable charging currents can be distinguished, and that the soma is charged with a time constant approximately equal to the access resistance times the somatic capacitance. Thus, the charging time of the soma is similar to what it would be if the cell had no process. Simple formulas were derived that can be used to calculate the electrotonic length, the membrane time constant, and the soma–dendrite resistance ratio of a cell with a cylindrical process. With the aid of these formulas, reasonable estimates of parameter values were recovered from simulated transient currents. Tests of the Rall model were proposed to determine when there is an equivalent cylinder that is consistent with observed charging behavior. The analysis was extended to a cable with an open end and to a model in which the soma and dendrite have different membrane time constants. It was shown that with voltage–clamp data estimates of electrical parameters other than ρ are relatively insensitive to differences between the membrane properties of the soma and dendrite. The methods of cable analysis introduced here were illustrated by application to charging transients recorded from a hippocampal pyramidal cell and from a neurohypophysial nerve ending. The Rall model provided a good description of the pyramidal cell current transient but was inconsistent with the charging behavior observed for the nerve ending. With the recent technical advance of patch clamp recording in brain slices, the analysis presented here should help neurophysiologists investigate cable properties in a wide variety of systems.

INTRODUCTION

Cable analysis has long been used to provide information about the electric and geometric properties of excitable cells. The shape of a cell and, in particular, the length and extensiveness of its branching dendrites determine the passive electrical response to a stepwise change in current or voltage. The shape of a dendrite also influences how a neuron responds to and integrates synaptic inputs. Thus, cable properties are important to the physiological function of a neuron and impinge on how a neuron performs as part of a complex nervous system. Cable analysis has an additional technical value in gauging the response time and spatial uniformity of a voltage clamp.

Data for cable analysis have almost always been obtained with sharp microelectrodes, primarily in a current-clamp circuit. There has been very little cable analysis with the patch-clamp technique. A few recent studies have used the patch clamp to obtain current-clamp data for cable analysis (Coleman and Miller, 1989; Pongracz et al., 1991). The patch clamp has not been used for cable analysis in the whole-cell voltage-clamp mode (cf. Llano et al., 1991), despite the fact that the voltage clamp may be advantageous in some respects (Rall, 1969; Stafstrom et al., 1984). One reason that the patch clamp has not been used much for cable analysis is that until recently it was technically difficult to apply the patch clamp to neurons in intact central nervous system (CNS) tissue. Recent successes at patch clamping neurons in brain slices have changed that (Blanton et al., 1989; Edwards et al., 1989). It is now possible to obtain low-access-resistance, high-resolution voltage-clamp recordings in visually identified neurons from virtually any brain region. These technical advances should greatly stimulate interest in using the patch clamp for cable analysis.

There has been a considerable amount of theoretical work on problems relevant to the use of electrophysiological techniques in the determination of cable properties (Rall, 1977; Jack et al., 1983; Rall and Segev, 1985). However, there has been relatively little attention to the theoretical problems specific to the conditions that pertain in the use of the whole-cell or tight-seal voltage-clamp. The relevant model is a voltage clamp with a low access resistance in a recording from a "Rall motoneuron." A Rall motoneuron is defined as having a cell soma with lumped RC behavior and a cylindrical process emanating from the cell soma. The finite-access-resistance variation has been discussed briefly by Rall (1969). The present investigation begins with a more detailed examination of this problem and develops a

0006-3495/92/03/756/11 $2.00

strategy for the application of the Rall motoneuron model to patch-clamp data.

To illustrate the application of this theory, data were obtained with the tight-seal voltage clamp from hippocampal pyramidal cells and from neurohypophysial nerve endings. The analysis of these data yielded estimates of cable parameters and indicated whether or not the Rall model was capable of describing the observed charging behavior.

RALL MODEL

The complex geometry of motoneurons and of many other neurons is often represented approximately as a lumped RC element in parallel with a cylindrical process of finite length (Fig. 1; Rall, 1969; Jack and Redman, 1971; Jack et al., 1983). The lumped RC component corresponds to a nerve cell body that may not be spherical but is for all practical purposes isopotential. It has been shown by Rall (1959) that even a very extensively branched dendrite reduces mathematically to this simpler model, provided that segments are cylindrical, that branches obey the 3/2 power law, and that the branches terminate at equivalent electrotonic lengths. Although analysis with much more elaborate compartmental models is widely used (Segev et al., 1989), the Rall model is still very useful as the starting point in a study and in providing the most basic electrical parameters. For the geometric situation of a roughly spherical presynaptic nerve ending at the end of an axon, the basic geometry is the same as for the Rall model, and this paper will also consider the applicability to data from such a system.

The basic mathematical strategy in dealing with this problem is well established. The following analysis follows that of Rall (1969) but focuses exclusively on the finite-access-resistance case and develops it more fully. Within a cylindrical cable in which radial gradients are negligible, voltage versus time and position satisfy the cable equation

$$\frac{\partial V}{\partial T} = \frac{\partial^2 V}{\partial X^2} - V,$$

as expressed in terms of the dimensionless variables $X = x/\lambda$ and $T = t/\tau_m$. V is voltage, x is the distance along the axis of the cylinder, t is time, λ is the length constant of the cylinder, and τ_m is the membrane time constant. A general solution of the cable equation is

$$V = [A \sin(\alpha X) + B \cos(\alpha X)]e^{-(1+\alpha^2)T}. \quad (1)$$

Determining a specific solution involves finding a set of A_i, B_i, and α_i that is consistent with the boundary and initial conditions. For a cylinder of finite length there are two boundary conditions, one at each end. At the end comprising the cell body, the boundary condition for the low-access-resistance voltage clamp can be formulated by examining the diagram of a patch-clamped motoneuron shown in Fig. 1 and by considering all contributions to current. The current through the patch electrode is $V_c/R_a - V_0/R_a$, where V_c and V_0 are command and soma voltages, respectively, and R_a is the access resistance (Fig. 1). The capacitance charging current of the soma is $-C_s\partial V_0/\partial t$, where C_s is the soma capacitance. A current V_0/R_s flows across the soma membrane; R_s is soma resistance. An axial current $1/(r_i\lambda)\ \partial V/\partial X$ flows into the cable (r_i is the cytoplasmic axial resistivity; the derivative is evaluated at $X = 0$). Since these various contributions to current add up to zero, we have as the boundary condition at $X = 0$ (Rall, 1969)

$$\rho_\infty \frac{\partial V_0}{\partial X} = (R + 1)V_0 + \frac{\partial V_0}{\partial T}, \quad (2)$$

where $R = R_s/R_a$ and $\rho_\infty = R_s/(r_i\lambda)$ (the soma-to-cable resistance ratio that the cell would have if the cable had an infinite length). The term $-RV_c$ can be neglected for a pulse to $V_c = 0$. Note that $\rho_\infty \tanh(L) = \rho$, where L is the electrotonic length of the cylinder.

The other boundary condition is at the distal end of the cable, where $X = L$. The cable is considered to be closed so that no current flows in the axial direction at

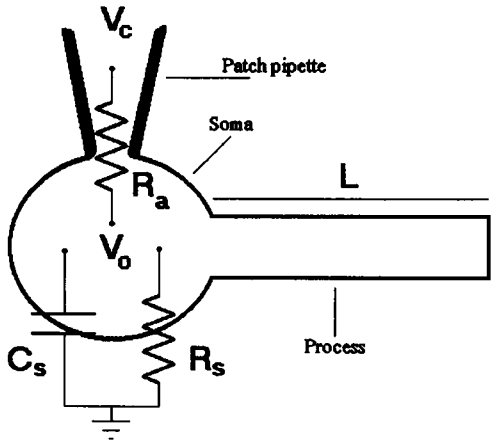

FIGURE 1. Diagram of a tight-seal voltage-clamped Rall motoneuron. V_c is controlled by a patch-clamp amplifier and is connected to V_0 by R_a. Current flows across R_s and C_s, and down the attached process, which is modeled as a finite cylinder of electrotonic length L, with a sealed end.

$X = L$. This prescribes a boundary condition of

$$\frac{\partial V_L}{\partial X} = 0. \tag{3}$$

If there were no access resistance, so that the clamp was acting at $X = 0$, the solution to the cable equation (Eq. 1) could be restricted to terms of the form $A_i \sin(\alpha_i X)$, with all the cosine terms zero. The reason for this is that at $X = 0$ there can be no change in V with time for a set V_c. The sine terms, being identically zero at $X = 0$, satisfy the mathematical requirement that V_0 is constant. With a finite access resistance, V_c can be constant, but V_0 must be allowed to change. This forces the cosine coefficients, B_i, to be nonzero. As the series resistance becomes larger, the voltage clamp becomes poorer and the cosine terms become larger.

Substituting Eq. 1 into Eq. 2 to impose the boundary condition at the soma, we have $A\alpha\rho_\infty = B(R - \alpha^2)$. Substituting Eq. 1 into Eq. 3 to impose the boundary condition at $X = L$ leads to

$$A = B \tan(\alpha L). \tag{4}$$

Combining these two results leads to

$$\tan(\alpha L) = \frac{R - \alpha^2}{\alpha\rho_\infty} = \frac{A}{B}, \tag{5}$$

the solutions of which define the eigenvalues of the system, α_i. With the aid of Eq. 4 the ratio A_i/B_i is then determined for each α_i, but the values of A_i and B_i depend on the initial $V(X)$ at $T = 0$. Note that the first part of Eq. 5 is identical to Eq. 45 of Rall (1969), which was derived using only a sine series.

Eq. 5 defines the time constants of the charging current. Fig. 2 illustrates the essential behavior of this transcendental equation in plots versus α for $R = 300$, $\rho_\infty = 2$, and three different values of L. These plots reveal the relevant properties of Eq. 5 and help to convey the physical significance of the different eigenvalues of the system. It is clear from Fig. 2, as well as from inspection of Eq. 5, that many eigenvalues are approximately given by

$$\alpha_i \cong (2i - 1)\frac{\pi}{2L}, \tag{6}$$

with $i \geq 1$. This approximation improves as R increases and is excellent for $R > 100$. Since $R > 100$ can be routinely achieved with the patch clamp in whole-cell recording, Eq. 6 is readily applicable to such experiments. The factors that produce errors in Eq. 6 will be discussed below.

Roots of the form dictated by Eq. 6 lead to time

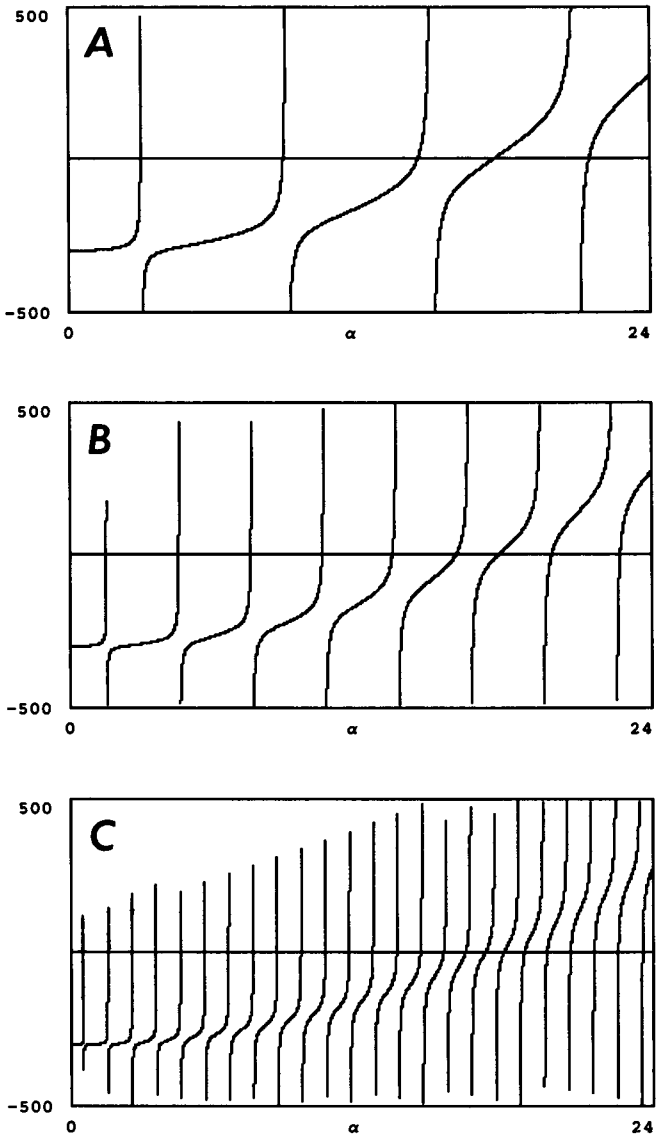

FIGURE 2. Plots of $\rho_\infty\alpha \tan(\alpha L) - R + \alpha^2$ vs. α to show the roots of Eq. 5. All plots are for $R = 300$ and $\rho_\infty = 2$, and $L = \pi/6$ (A), $L = \pi/3$ (B), and $L = \pi$ (C). Note that most crossings of the α axis occur at values dictated by Eq. 6. But for α near $\sqrt{R} = 14.1$, the roots are clearly not close to the asymptotes of the tangent function at half-integral multiples of π/L.

constants of the form

$$\tau_i = \frac{\tau_m}{1 + \left[\frac{(2i - 1)\pi}{2L}\right]^2}, \tag{7}$$

which follows from Eq. 6 and the fact that $T = t/\tau_m$. L can then be calculated from the two slowest time

constants as

$$L = \frac{\pi}{2}\sqrt{\frac{9 - R_\tau}{R_\tau - 1}}, \quad (8)$$

where $R_\tau = \tau_1/\tau_2$. Note that Eqs. 6, 7, and 8 are essentially identical to Eqs. 29, 32, and 33, respectively, in Rall (1969).

While most of the eigenvalues are half-integral multiples of π/L (Eq. 6), there is one eigenvalue, $\alpha_R^2 \cong R$, that has fundamentally different properties from the other roots of Eq. 5. This root, which will be denoted as α_R, yields a time constant of $\sim R_a C_s$, which is the well-known charging time for a voltage clamp of a spherical cell (Sigworth, 1983). The fact that a time constant of the form $R_a C_s$ falls out of the analysis of a neuron with a cylindrical process is an important and noteworthy result. This means that the transient cancelation method for determining R_a and C_s, as is done routinely in patch-clamp experiments, is applicable not only to the spherical cell analyzed in the original development of the tight-seal voltage clamp, but also for the more complex cell geometry of the Rall motoneuron. This is good news for patch clampers, provided that they know which component of the charging transient corresponds to this particular eigenvalue of the system.

To determine which exponential component corresponds to the eigenvalue α_R, and thus which component has the time constant $R_a C_s$, it is instructive to examine the amplitudes of the different exponential components of charging current. The cosine terms are related directly to measured transient current by the relationship $W_i = B_i/R_a$, where W_i is the amplitude of component i. Eq. 4 suggests that $B_i \ll A_i$ for the eigenvalues that are near $(2i - 1)\pi/2L$. Only for α_R, which is not near a half-integral multiple of π/L, can the cosine coefficient B_R be as large as or larger than the sine coefficient A_R. Since B_R should be much larger than the other cosine coefficients, it is then reasonable to expect that the component of current with the time constant $R_a C_s$ will be much larger than the other exponential components. This has been observed both in experiments and in simulations (see below). A large amplitude thus provides a practical basis for distinguishing the somatic component from the other components of the charging transient.

The component with time constant $R_a C_s$ is in essence a current that charges the soma, whereas the slower components, corresponding to the eigenvalues of the form of Eq. 6, are in essence cable charging current. Although there is inevitably some mixing, it is still useful to refer to the components in this way as soma charging and cable charging, and this terminology will be used below.

At this stage two useful tests of the Rall model can be pointed out. The time constants associated with cable charging should, according to this analysis, be virtually insensitive to the access resistance, as long as the resistance ratio R is large. Only α_R should vary with R_a. This is in marked contrast to the two-compartment model used by Llano et al. (1991) to analyze charging transients of patch-clamped cerebellar Purkinje cells. The two-compartment model predicts a charging current with two exponentials, both of which are dependent on R_a. Thus, by changing the degree of series resistance compensation, data can be collected from the same cell with different values of R_a. In this way the two-compartment model can be tested versus a model of a neuron with a cylindrical process.

Another useful test of the equivalent cylinder representation arises from Eq. 8, which indicates that the ratio of the two slowest time constants of the charging transient cannot exceed 9.

$$R_\tau < 9 \quad \text{(Ineq. 1)}$$

Violation of this inequality would have to be taken as evidence that there is no equivalent cylinder that can account for the observed transient.

Fourier coefficients

A set of A_i and B_i must be found that produces a Fourier sum equal to the steady-state solution:

$$V(X) = V_0 \frac{\cosh(L - X)}{\cosh(L)} = \sum [A_i \sin(\alpha_i X) + B_i \cos(\alpha_i X)], \quad (9)$$

which, with the aid of Eq. 4, becomes

$$V(X) = V_0 \frac{\cosh(L - X)}{\cosh(L)} = \sum \left[\frac{A_i \cos \alpha_i (L - X)}{\sin(\alpha_i L)}\right]. \quad (10)$$

Fourier transformation is not strictly valid because these cosine functions are not an orthogonal set. However, the set of cosine functions with α defined as half-integral multiples of π/L does form an orthogonal set over the interval $[0, L]$. Thus, we can proceed by assuming orthogonality for all trigonometric functions in Eq. 10 except that with α_R. The additional concern that the eigenvalues are only approximately half-integral multiples of π/L, and the consequence of this approximation on the orthogonality of the cosine functions, is taken up in the Appendix. Multiplying Eq. 10 by $\cos \alpha_i(L - X)$, integrating from 0 to L, and rearranging

gives

$$V_0 \frac{\alpha_i}{1+\alpha_i^2} - \frac{A_R \alpha_i \cot(\alpha_R L)}{\alpha_i^2 - \alpha_R^2} \cong \frac{LA_i}{2\sin(\alpha_i L)} \cong \frac{LA_i}{2}, \quad (11)$$

where the final approximation follows from Eq. 6. Since $\alpha_R \gg \alpha_i$ for small i, we can ignore the second term on the left side of this expression, provided that $A_R \cot(\alpha_R L)$ is not large. Since α_R is not near values specified by Eq. 6, this last provision is reasonable. Despite the simplicity of Eq. 11, it is not yet useful because, as already noted, the amplitudes of the measured current transient are $W_i = B_i/R_a$. To get an expression for B_i, we use Eqs. 4 and 5 to obtain from Eq. 11

$$V_0 \frac{\alpha_i}{1+\alpha_i^2} \cong \frac{L B_i (R - \alpha_i^2)}{2\alpha_i \rho_\infty}.$$

Replacing ρ_∞ by $R_s/R_{c\infty} = R_s/R_c \tanh(L)$, where R_c is the cable resistance measured at $X = 0$ and $R_{c\infty} = R_c \tanh(L)$ is the resistance for a cable of infinite length; replacing R by R_s/R_a; and noting that $R - \alpha_i^2 \cong R$ for the smaller α_i leads to an expression for the observed amplitudes

$$W_i \cong \frac{2V_0 \alpha_i^2}{R_c L \tanh(L)(1+\alpha_i^2)}. \quad (12)$$

The accuracy of this expression will be examined in simulations described below. On the basis of arguments given in the Appendix and the results of the simulations, Eq. 12 is reasonably accurate for α_1. This provides a useful expression for the cable resistance

$$R_c = \frac{2V_0 \alpha_1^2}{W_1 L \tanh(L)(1+\alpha_1^2)}, \quad (13)$$

where α_1 is simply $\pi/2L$. Thus, with L estimated from Eq. 8, R_c can be determined. Since R_s can be obtained from C_s and τ_m, we can compute the important quantity $\rho = R_s/R_c$. This constitutes a complete strategy for estimating the essential parameters of the Rall model from experimental patch-clamp data.

Note that for a finite cylinder $R_c = R_m/\pi d\lambda \tanh(L)$ and $C_c = \pi d\lambda C_m \tanh(L)$. C_c is defined as Q_c/V_0. Q_c is the charge, integrated along length of the cable, that produces the steady-state voltage distribution (Eq. 10) when the voltage at $X = 0$ is V_0, d is the cable diameter, and R_m and C_m are the resistance and capacitance, respectively, of unit areas of membrane. Thus, with $R_c C_c = R_m C_m = \tau_m = \tau_1(1+\alpha_1^2)$, we obtain from Eq. 12

$$\frac{W_1 \tau_1}{2C_c V_0} \cong \frac{\alpha_1^2}{(1+\alpha_1^2)^2 L \tanh(L)}. \quad (14)$$

The right-hand side of Eq. 14 is a monotonically decreasing function of L with a maximum of $(2/\pi)^2 = 0.405$ as L goes to zero. This implies the inequality

$$\frac{W_i \tau_1}{C_c V_0} < 0.81 \quad \text{(Ineq. 2)}$$

The left side of this inequality is the ratio of the charge carried by the slowest component of the cable charging transient to the total charge that charges the cable capacitance. Thus, for a Rall motoneuron, the fraction of total cable charging current contributed by the slowest component cannot exceed 81% and decreases as L becomes longer.

Estimating C_s and R_a

The somatic component of the charging transient will have a short time constant of $\sim R_a C_s$ and will have a larger amplitude than the other components. In voltage-clamp experiments from this laboratory on hippocampal pyramidal cells and neurohypophysial nerve endings, it was easy to see this fast somatic component, with a time constant ranging from 5 to 200 μs and an amplitude of the order of 2 nA for a 10-mV step. Slower components of transient current associated with cable charging were generally much smaller and never exceeded 500 pA. The values of R_a determined by balancing out this large fast component with the circuitry of the patch-clamp amplifier were in line with values normally obtained in patch-clamp studies of spherical cells (Marty and Neher, 1983) and were generally correlated with the initial resistance of the patch electrode. The values of C_s obtained from cells with processes were also in the same range as values obtained from spherical cells and were generally correlated with visual estimates of size. The pyramidal cells from 1-wk-old rats yielded C_s values in the range of 5 to 20 pF, whereas the smaller nerve endings of the posterior pituitary had an average C_s of 2 pF (Jackson, unpublished observation). In simulations described below a component of current with the correct time constant dominated the transient. Thus, the large fast component of the charging transient is a reasonably well-isolated soma charging current with a time constant of $R_a C_s$.

The accuracy of estimates of R_a and C_s from transient balancing depends partly on how well $\alpha_R^2 \cong R$ approximates a root of Eq. 5. An additional error arises when one adjusts the potentiometers of a patch-clamp amplifier to eliminate the somatic component, even if α_R^2 is exactly R. The apparent access resistance and soma capacitance (indicated by the subscript x) are related to the real R_a and C_c as follows. $W_R = V_0/R_x$, and the total initial current is given by $V_0/R_a = W_R + \Sigma W_i$ (the sum is over all observed components except W_R). It then

follows that

$$R_a = \frac{V_0}{\frac{V_0}{R_x} + \Sigma W_i} \tag{15a}$$

This equation provides an improved estimate of R_a from the apparent value, R_x, and the amplitudes of the other components. It is clear that when the cable components are small, then so is the difference between R_x and R_a. The relationship

$$C_s = \frac{\tau_R}{R_a} = \frac{R_x C_x}{R_a} \tag{15b}$$

can be used to compute C_s from C_x, R_x, and R_a.

Estimating L, τ_m, and ρ

A procedure involving the use of Eqs. 7 and 8 to determine L and τ_m has been suggested by Rall (1969). With C_s estimated by the transient balancing procedure, and possibly corrected by Eqs. 15, a and b, R_s can readily be computed as τ_m/C_s. R_c can be estimated from L with Eq. 13, and ρ is then the ratio.

Eqs. 7 and 8 indicate that L and τ_m can be determined when the two slowest time constants are well approximated by Eq. 6. It is then instructive to return to Eq. 5 and ask under what conditions Eq. 6 will be accurate for $i = 1$ and 2. Examination of plots such as Fig. 2 for a wide range of parameters showed that the roots of Eq. 5 deviate from Eq. 6 as α approaches $\alpha_R = \sqrt{R}$. These plots indicate that for $R > 100$ only the root flanking α_R is noticeably distorted. Thus, we need three roots below α_R for Eq. 6 to be accurate for $i = 1$ or 2. We can apply this condition by setting $i = 4$ and obtaining from Eqs. 5 and 6 the condition

$$\sqrt{R} > \alpha_4 = \frac{7\pi}{2L}$$

or

$$R > \frac{121}{L^2}.$$

When this condition is not satisfied, then Eq. 6 may not approximate the two slowest time constants well, and the above-outlined strategy of estimating L and τ_m may not be reliable. Examination of plots of Eq. 5 indicates that Eq. 6 is less sensitive to ρ_∞, but it is more difficult to propose a criterion comparable to that given above for R and L. In general, as ρ_∞ increases, Eq. 6 becomes a poorer approximation.

A useful check can be implemented by computing the resistance of the whole cell, R_w, as two resistances in parallel,

$$\frac{1}{R_w} = \frac{1}{R_s} + \frac{1}{R_c}, \tag{16}$$

and comparing with the value computed with Ohm's law from the steady-state current.

If the membrane time constant is the same in the soma and cable, then $\tau_m = R_c C_c = R_s C_s$. Combining with Eq. 16 yields the expression $\tau_m = R_w(C_c + C_s)$, which is equivalent to

$$\tau_m = R_w C_w. \tag{17}$$

C_w is defined similarly to C_c in terms of the charge that produces the steady-state voltage distribution. Eq. 17 is applicable to a general class of sealed processes with a uniform membrane, in which the voltage can be expressed as a function of a single variable X. The total charge needed to produce a given steady-state voltage $V(X)$ is proportional to the integral of $V(X)$ over X. The steady-state current is inversely proportional to the same integral. This geometry-specific integral drops out of the product, leaving $\tau_m = R_c C_c$. This result can easily be extended to a cell with many such processes in parallel. This is valid for a very general set of assumptions and is therefore relatively model independent. Unfortunately, Eq. 17 is not very useful because, as with C_c, C_w does not relate to a time constant of the system and so cannot be measured directly. C_w is also not simply related to the area of the transient, and estimating the total capacitance charge in this way is an error.

SIMULATION OF CURRENT TRANSIENTS

To test the effectiveness of the above-outlined strategy for obtaining cable parameters from voltage-clamp experiments, and to test some of the mathematical approximations, the cable equation was integrated numerically and the resulting simulated charging transients were analyzed. A program was written in *C* for this purpose. This program employed the Euler-forward procedure, incorporating boundary conditions by using the "centered-difference" formula (Mascagni, 1989). To compensate for the poor performance of the Euler-forward method, small step sizes were used (stiffness parameter <0.2). The transients were analyzed by fitting to a sum of four exponentials, using a weighting function of exp $(-2T)$.

The soma charging current generally had an amplitude that was far larger than the amplitudes of the cable charging components. The time constant of the soma charging component was very near the value expected for $\alpha_R^2 = R$. The parameters L, τ_m, and ρ were estimated as outlined above from the two slowest time constants of

the transient and the amplitude of the slowest component. The results are presented in Table 1 for simulations with $R = 100$, $L = 1$ and 2, and $\rho_\infty = 1$ and 5.

The parameters recovered from the simulated transients were reasonably close to the starting values when one considers the number of parameters that it was necessary to fit. It is interesting that the largest deviations were observed for $L = 1$ and $\rho_\infty = 5$. For these values, the approximation of the eigenvalues as half-integral multiples of π/L would be expected to be the poorest. The recovery of reasonable values for ρ_∞ suggests that the approximations used to derive Eqs. 12 and 13 are adequate for $i = 1$. In general, the amplitudes W_i increased with i (Eq. 12). However, the values recovered for W_2 and τ_3 were often a factor of two from the expected values, indicating that with $R = 100$, there can be problems with Eq. 12 for $i = 2$ and with Eq. 6 for $i = 3$. The situation would be expected to improve for larger R, but simulation and analysis were difficult because of the wide range of time scales involved.

OPEN-END CABLE

The analysis of the open-end cable differs from that of the closed-end case only in the boundary condition at $X = L$. Instead of Eq. 3, we have $V_L = 0$. Analysis similar to that which led to Eq. 5 yields

$$-\cot(\alpha L) = \frac{R - \alpha^2}{\alpha\rho_\infty} \tag{18}$$

as the transcendental equation that defines the eigenvalues. The eigenvalues are now of the form

$$\alpha \cong \frac{i\pi}{L} \tag{19}$$

TABLE 1 Parameter estimates from simulated currents

	$\rho_\infty = 1$	$\rho_\infty = 5$
$L = 1$	$L = 1.03$	$L = 1.22$
	$\tau_m = 0.97$	$\tau_m = 0.82$
	$\rho_\infty = 1.18$	$\rho_\infty = 8.2$
$L = 2$	$L = 1.73$	$L = 1.72$
	$\tau_m = 1.13$	$\tau_m = 1.16$
	$\rho_\infty = 0.87$	$\rho_\infty = 4.9$

The cable equation was integrated numerically with the boundary conditions as stated in Eqs. 2 and 3. The ratio of the soma resistance to the access resistance, R, was taken as 100. The membrane time constant (τ_m) for these simulations was 1. ρ_∞ was 1 or 5 as indicated in the column headings; L was 1 or 2 as indicated in the row headings. R_a and C_s were determined from the time constant and amplitude of the fastest component and corrected with Eqs. 15a and 15b. L, τ_m, and ρ_∞ were calculated from τ_1, τ_2, and W_1 using Eqs. 7, 8, and 13, as described in the text.

with $i \geq 1$. As with the analysis above, there is a root $\alpha_R^2 \cong R$, to give a time constant of $\sim R_a C_s$. Continuing the analysis as above for a process with a closed end, the time constants have the form

$$\tau_i = \frac{\tau_m}{1 + \left(\frac{i\pi}{L}\right)^2}. \tag{21}$$

The expression for L in terms of the ratio of the two slowest time constants is then

$$L = \pi\sqrt{\frac{8 - R_\tau}{R_\tau - 1}}, \tag{22}$$

which is quite similar in form to the expression for L for the closed-end model (Eq. 8). This indicates that $R_\tau < 8$, compared with 9 for the closed-end model (Ineq. 1). Further analysis similar to that employed above to obtain Fourier coefficients for the closed-end system, and making essentially the same approximations, yields Eq. 12 again, except that α_i are given by Eq. 19. When the right side of Eq. 12 is evaluated for different values of L but with α_1 as π/L, it can be seen that the quantity $W_i\tau_1/2C_cV_0$ then approaches 0.069 as L approaches zero and has a maximum of 0.088 at $L = 1.8$.

PERFORATED SOMA/INSULATING SOMA

The perforated soma model was introduced out of concern over the possibility of an electrical shunt resulting from microelectrode penetration (Durand, 1984; Kawato, 1984). The partial short circuit is thus treated mathematically as a lower resistivity of the soma membrane. With the tight-seal whole-cell voltage clamp, the opposite may occur. The washout of channels could raise the resistivity of the soma membrane, resulting in an "insulating soma." Aside from these technical questions, there is an important scientific question as to whether the membranes of the cell soma and dendrite have different properties (Pongracz et al., 1991). These considerations have motivated the following analysis, which incorporates differences in resistivity of the somatic and dendritic membranes.

The formulation differs from that of the Rall motoneuron above only in the boundary condition at $X = 0$ (Eq. 2), which is changed to

$$\rho_\infty \frac{\partial V_0}{\partial X} = (R + 1)V_0 + \frac{\tau_s}{\tau_c}\frac{\partial V_0}{\partial T}, \tag{23}$$

where τ_s and τ_c are the time constants of the soma and cable membranes, respectively. The eigenvalues of the

system are then defined by the expression

$$\alpha\rho_\infty \tan(\alpha L) = R + 1 - \frac{\tau_s(1+\alpha^2)}{\tau_c}, \qquad (24)$$

and the roots of this equation are once again given approximately by Eq. 6. Thus, Eq. 8 can still be used to calculate L. Eq. 7 would then yield τ_c because T is now in units of τ_c. The soma charging time constant C_sR_a still emerges, because for large R, $\alpha^2 \cong R\tau_c/\tau_s = \tau_c/R_aC_s$ is an approximate root of Eq. 24. It is significant that L and τ_c can be determined in the same way as for the standard Rall model. As long as the ratio of soma and cable membrane time constants is much smaller than the ratio of the soma resistance to the access resistances ($R \gg \tau_s/\tau_c$), the cable charging time constants, and estimates of L and τ_m, are not significantly altered by differences in resistivity between the soma and cable membranes. This insensitivity of cable parameters estimated from voltage-clamp data was also noted by Rall (1969) and is in marked contrast to the current-clamped perforated-soma model, where the shunt can seriously alter estimates of L (Pongracz et al., 1991).

The analysis of the Fourier coefficients was not altered by allowing the cable and soma resistivities to be different. Eq. 12 is valid under the present conditions, leading to Eq. 13 as well. Thus, R_c can be estimated once L has been computed from Eq. 8. R_s cannot be determined from C_s in this model because the soma membrane time constant τ_s is not yet known. Thus, ρ must be determined differently. Eq. 16 can be used to estimate R_s from R_c and the whole-cell resistance R_w. Whereas Eq. 16 was an "extra" relationship above, which provided a check of internal consistency for the Rall model, the additional parameter in the present model removes this constraint. If the assumption of a uniform membrane time constant leads to a computed value of R_w that diverges from the value measured from the steady-state current, the perforated soma/insulating soma model may be implicated as a plausible alternative.

EXPERIMENTS

Methods

Patch-clamp recordings were made in thin slices using the method of Edwards et al. (1989). Recordings were made with EPC-7 or EPC-9 patch clamp amplifiers (Instrutech, Elmont, NY). Transient cancellation was implemented by manual adjustment of the amplifier potentiometers to determine R_a and C_s. Voltage steps were applied to the same cell, with or without series resistance compensation. Hippocampal slices 100 μm thick were prepared from 1-wk-old rats. Posterior pituitary slices 80 μm thick were prepared as described by Jackson et al. (1991) from 2-mo-old rats.

From a holding potential of −90 mV, the voltage was stepped to −100 mV for 10 or 20 ms, then to −80 mV, then back to −90 mV. The pulse protocol was repeated 50 times at a repetition rate of ~5 Hz. The charging transients were averaged and fit to sums of exponentials with the program REVIEW (Instrutech). The −90 to −100 mV response and the −80 to −90 mV responses were frequently compared and found to be identical. The −100 to −80 mV response was twice the response for the 10-mV steps with amplitudes proportionally larger.

The parameters L and τ_m were computed for the Rall model by using Eqs. 7 and 8. R_c was determined from L by Eq. 13, which then made it possible to compute ρ.

Pyramidal cells

Fig. 3 shows the average of 50 current responses to voltage pulses for a pyramidal cell in the CA1 region of the hippocampus. The recording was made with 54% series resistance compensation. The fastest component had been removed with the transient cancellation circuitry of the patch-clamp amplifier. A sum of three exponentials provided an excellent fit to the remaining transient. The parameters are given in the figure legend. The fit to a sum of four exponentials did not reduce the

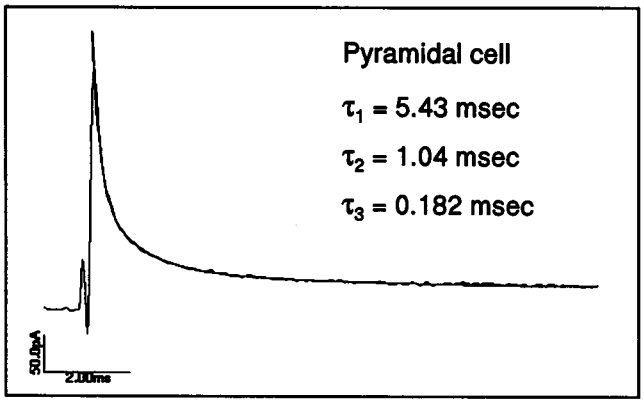

FIGURE 3. Charging current recorded from a voltage-clamped pyramidal cell (average of 50 responses). The best fitting sum of three exponentials was also drawn and overlies the data. The time constants were (in ms) $\tau_1 = 5.43$, $\tau_2 = 1.04$, and $\tau_3 = 0.182$; and the weights were (in pA) $W_1 = 20.5$, $W_2 = 111$, and $W_3 = 462$. The soma capacitance was 14.9 pF, and the series resistance was 9.5 MΩ, as estimated from balancing the fastest component of the transient. Series resistance compensation was 54%. L was estimated as 1.49 from Eq. 8; τ_m was 11.5 ms from Eq. 7. ρ was 1.6, with R_c estimated with Eq. 13 as 380 MΩ. With R_s estimated as 610 MΩ, R_w was computed to be 230 MΩ from Eq. 16 and 330 MΩ from the steady-state current and Ohm's law.

sum-of-squares error, while the best-fitting sum of two exponentials showed clear deviations from the experimental data and a larger sum-of-squares error. The time constants for cable charging were not significantly different from those of a transient recorded from the same cell without series resistance compensation.

Parameters computed from the time constants and amplitudes are shown in the legend of Fig. 3. R_w computed from R_s and R_c with Eq. 16 was 230 MΩ, which compares favorably with the value of 330 MΩ obtained from Ohm's law. The amplitudes of the exponential components increased with i, as expected from Eq. 12, but the results of the simulation suggest that caution is necessary in interpreting the values of these quantities for $i \geqslant 2$. All in all, an equivalent cylinder model provides a reasonable description of the charging of this pyramidal cell. Although studies in neurons from adult hippocampus indicate that the processes do not satisfy the equivalent cylinder model (Turner and Schwartzkroin, 1980), the situation could be different in neurons from a very young animal. The present analysis is intended for illustration of the method, not for comparisons with other studies (Turner and Schwartzkroin, 1980; Brown et al., 1981). A more extensive study will be required to make a more general statement about pyramidal cells in this particular preparation.

Posterior pituitary nerve terminals

Fig. 4 shows the average of 50 current responses to voltage pulses for a posterior pituitary nerve ending. The recording was made with 60% series resistance compensation. As with the pyramidal cell above, a sum of three exponentials provided the best fit to the transient that remained after cancellation of the fastest component. The time constants for cable charging were not significantly different from those of a transient recorded from the same nerve ending without series resistance compensation. The ratio of the two slowest time constants was 12.8, violating Ineq. 1. Thus, the charging transient is not consistent with a Rall model, and L could not be computed. This result could be due to a complex geometry of the axon leading to this nerve ending. Anatomic studies have shown that these axons branch into a large number of nerve endings (Nordmann, 1977). Biocytin labeling in this preparation has revealed multiple swellings along the axon (Jackson, unpublished observation).

Note that $W_1 > W_2$. Thus, in contrast to what was found for the pyramidal cell examined above, a qualitative prediction of Eq. 12 was violated. This can be taken as additional evidence that the process does not have a suitable equivalent cylinder representation.

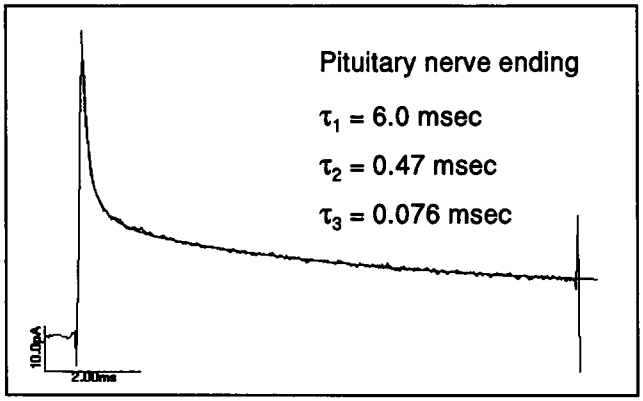

FIGURE 4. Charging current recorded from a voltage-clamped neurohypophysial nerve ending (average of 50 responses). The best-fitting sum of three exponentials was also drawn and overlies the data. The time constants were (in ms) $\tau_1 = 6.0$, $\tau_2 = 0.47$, and $\tau_3 = 0.076$; and the weights were (in pA) $W_1 = 15.1$, $W_2 = 11.8$, and $W_3 = 89$. The terminal capacitance was 2.2 pF, and the series resistance was 7.5 MΩ. Series resistance compensation was 60%. The ratio $\tau_1/\tau_2 = 12.8$, thus violating Ineq. 1 and indicating that an equivalent cylinder model cannot account for the observed transient.

DISCUSSION

With the development of techniques for patch-clamp recording in brain slices (Blanton et al., 1989; Edwards et al., 1989), cable theory of the finite-access-resistance voltage clamp should be very useful. Patch-clamp techniques can be used in virtually any region of the CNS to record charging transients from visually selected neurons of many different types and morphologies. The cable charging transients obtained with the tight-seal whole-cell voltage clamp typically have the two slow exponential components needed for this analysis.

The mathematical separation of the soma charging current from the cable charging current was particularly advantageous. This separation has some significant technical implications. First, the transient cancellation procedure used as a standard practice in patch-clamp experiments is justified and informative even when cells have large cylindrical processes. Second, somatic membrane currents can be recorded with temporal resolution comparable to that achieved in cells lacking processes, provided that active currents in processes are small and well behaved. Passive process charging can be assessed and, except when unusually large, will not appreciably compromise the time for charging of the soma. Needless to say, large voltage-activated currents in processes of significant length would still interfere with many kinds of voltage-clamp experiments, and no solution to this problem is proposed.

The analysis presented here suggests some electrophysiological tests to evaluate the widely used Rall model and determine whether there is an equivalent cylinder that is consistent with observed transient behavior. One test is whether or not the slowest charging time constants are altered by series resistance compensation. Cable theory predicts that for a high ratio of soma resistance to access resistance, the time constants for cable charging will be relatively insensitive to series resistance (Eqs. 6 and 7). In contrast, the slow time constant can become faster with increased series resistance compensation in a two-compartment model (Llano et al., 1991). Thus, comparisons of charging time constants in transients recorded with and without series resistance compensation can be useful as a means of distinguishing between such models.

Another test of the Rall model is suggested by the comparison of the resistance of the whole cell as determined from cable analysis (Eq. 16) with the value obtained from the steady-state current and Ohm's law. Agreement between values determined by different methods would suggest that the estimates are reliable and that the Rall model provides a consistent description. On the other hand, if a large discrepancy is found, the implication would be that the process does not have a suitable equivalent cylinder representation. Perhaps the strongest test of the Rall model is provided by Ineq. 1. If the ratio between the two slowest time constants is >9, then the transient cannot be accounted for by the charging of an equivalent cylinder.

There is, in principle, much more additional information contained in the six parameters obtained by fitting to the three exponentials normally observed. Unfortunately, the simulations and the nature of the approximations used in this analysis indicate that the amplitudes and time constants of the faster components of cable charging current cannot be used effectively in the analysis of such data. Nevertheless, a qualitative deviation from the expected behavior of the amplitude W_2, such as was described above for the pituitary nerve ending, is likely to result from the inadequacy of the equivalent cylinder model. In contrast to the transient recorded from a pituitary nerve ending, data from a hippocampal pyramidal cell showed reasonable agreement. While positive results with such tests can be useful in establishing consistency with the Rall model, failure of these tests is not easy to interpret. It is difficult to suggest what a better model might be or to make a statement about the geometry of a process for data that defy an equivalent cylinder interpretation. These tests will then probably be most valuable either to justify continued use of an equivalent cylinder representation or to indicate that a more elaborate compartmental analysis should be combined with anatomic studies (Segev et al., 1989).

APPENDIX

In the derivation of the fourier coefficients (Eqs. 10 to 12) it was assumed that the eigenvalues defined by Eq. 5, which are given approximately in Eq. 6, generate a set of cosine functions that are orthogonal in the interval [0, L]. Since Eq. 6 is approximate, the orthogonality is not exact. It is thus important to evaluate the error that can arise from this assumption. We begin with the integral

$$\int_0^L \cos \alpha_i(L - X) \cos \alpha_j(L - X)dX$$

$$= \frac{\tfrac{1}{2} \sin ((\alpha_i + \alpha_j)X)}{\alpha_i + \alpha_j} - \frac{\tfrac{1}{2} \sin ((\alpha_i - \alpha_j)X)}{\alpha_i - \alpha_j}$$

$$= \frac{1}{\alpha_i^2 - \alpha_j^2} \cos (\alpha_i L) \cos (\alpha_j L)$$

$$\cdot (\alpha_i \tan (\alpha_i L) - \alpha_j \tan (\alpha_j L)).$$

Using Eq. 5 to replace the tangent terms leads to

$$= -\frac{\cos (\alpha_i L) \cos (\alpha_j L)}{\rho_\infty}.$$

Since $\alpha_i L$ and $\alpha_j L$ are near half integral multiples of π, this final quantity is small, justifying the neglect of the overlap integrals in the derivation of the fourier coefficients. In fact, even if one of the α is somewhat poorly approximated by Eq. 6, the above result is a product of the cosines of both α, so the overlap integral will still be small. This indicates that Eqs. 12 and 13 for $i = 1$ should be accurate. On the other hand, if neither α_i nor α_j are small, Eqs. 12 and 13 may be much less accurate.

I am especially indebted to Matt Banks for many valuable comments on this manuscript and for the suggestion of the simulation study. I also thank Indira Raman, Kevin Ketchum, Bob Pearce, André Kooyman, Shuanglin Zhang, and Larry Trussell for their comments on this manuscript. The data from neurohypophysial nerve endings were obtained while the author was a guest in the laboratory of Dr. Arthur Konnerth at the Max Planck Institute for Biophysical Chemistry.

This research was funded by grants NS-23512 and NS-30016 from the National Institutes of Health.

Received for publication 2 August 1991 and in final form 6 November 1991.

REFERENCES

Blanton, M. G., J. J. Lo Turco, and A. R. Kriegstein. 1989. Whole cell recording from neurons in slices of reptilian and mammalian cerebral cortex. *J. Neurosci. Methods.* 30:203–210.

Brown, T. H., R. A. Fricke, and D. H. Perkel. 1981. Passive electrical constants in three classes of hippocampal neurons. *J. Neurophysiol. (Bethesda).* 46:812–827.

Coleman, P. A., and R. F. Miller. 1989. Measurement of passive membrane parameters with whole-cell recording from neurons in the intact retina. *J. Neurophysiol. (Bethesda).* 61:218–230.

Durand, D. 1984. The somatic shunt cable model for neurons. *Biophys. J.* 46:645–653.

Edwards, F. A., A. Konnerth, B. Sakmann, and T. Takahashi. 1989. A thin slice preparation for patch clamp recordings from neurons of the mammalian central nervous system. *Pflügers Arch.* 414:600–612.

Jack, J. J. B., and S. J. Redman. 1971. An electrical description of the motoneuron and its application to the analysis of synaptic potentials. *J. Physiol. (Lond.).* 215:321–352.

Jack, J. J. B., D. Noble, and R. W. Tsien. 1983. Electric Current Flow in Excitable Cells. Oxford University Press, London.

Jackson, M. B., A. Konnerth, and G. A. Augustine. 1991. Action potential broadening and frequency-dependent facilitation of calcium signals in pituitary nerve terminals. *Proc. Natl. Acad. Sci. USA.* 88:380–384.

Kwato, M. 1984. Cable properties of a neuron model with non-uniform membrane resistivity. *J. Theor. Biol.* 111:149–169.

Llano, I., A. Marty, C. M. Armstrong, and A. Konnerth. 1991. Synaptic- and agonist-induced excitatory currents of purkinje cells in rat cerebellar slices. *J. Physiol. (Lond.).* 434:183–213.

Marty, A., and E. Neher. 1983. Tight-seal whole-cell recording. *In* Single Channel Recording. B. Sakmann and E. Neher, editors. Plenum Press, New York. 107–121.

Mascagni, M. V. 1989. Numerical methods for neuronal modeling. *In* Methods in Neuronal Modeling. C. Koch and I. Segev, editors. MIT Press, Cambridge, MA. 439–484.

Nordmann, J. J. 1977. Ultrastructural morphometry of the rat neurohypophysis. *J. Anat.* 123:213–218.

Pongracz, F., S. Firestein, and G. M. Shepherd. 1991. Electrotonic structure of olfactory sensory neurons analyzed by intracellular and whole cell patch techniques. *J. Neurophysiol. (Bethesda).* 65:747–758.

Rall, W. 1959. Branching dendritic trees and motoneuron membrane resistivity. *Exp. Neurol.* 1:491–527.

Rall, W. 1969. Time constants and electrotonic length of membrane cylinders and neurons. *Biophys. J.* 9:1483–1508.

Rall, W. 1977. Core conductor theory and cable properties of neurons. *In* Handbook of Physiology. The Nervous System. Cellular Biology of Neurons. J. M. Brookhart and V. B. Mountcastle, editors. American Physiological Society, Bethesda, MD. 39–97

Rall, W., and I. Segev. 1985. Space-clamp problems when voltage-clamping branched neurons with intracellular microelectrodes. *In* Voltage and Patch Clamping with Microelectrodes. T. G. Smith, H. Lecar, S. Redman, and P. W. Gage, editors. American Physiological Society, Bethesda, MD. 191–215.

Segev, I., J. W. Fleshman, and R. E. Burke. 1989. Compartmental models of complex neurons. *In* Methods in Neuronal Modeling. C. Koch and I. Segev, editors. MIT Press, Cambridge, MA. 63–97.

Sigworth, F. J. 1983. Electronic design of the patch clamp. *In* Single Channel Recording. B. Sakmann and E. Neher, editors. Plenum Press, New York. 3–35.

Stafstrom, C. E., P. C. Schwindt, and W. E. Crill. 1984. Cable properties of layer V neurons from cat sensorimotor cortex in vitro. *J. Neurophysiol. (Bethesda).* 52:278–289.

Turner, D. A., and P. A. Schwartzkroin. 1980. Steady-state electrotonic analysis of intracellularly stained hippocampal neurons. *J. Neurophysiol. (Bethesda).* 44:184–199.